Progress Report

DEVELOPMENT OF PLUTONIUM-BEARING FUEL MATERIALS

October 1 through December 31, 1962
AEC R&D Contract AT(30-1)-2389

NUMEC P-103

Facsimile Price $ 4.60
Microfilm Price $ 1.52

Available from the
Office of Technical Services
Department of Commerce
Washington 25, D. C.

Nuclear Materials and Equipment Corporation
Apollo, Pennsylvania

For Official Use Only, Pending Patent Release

DISCLAIMER

External Distribution List

U. S. Atomic Energy Commission, New York Operations Office
- M. Balicki, Research and Development Division
- M. Plisner, Research Contracts and Technical Services Division
- H. S. Potter, Patent Group

U. S. Atomic Energy Commission, Washington
- S. Christopher, Division of Reactor Development
- R. Grube
- J. M. Simmons (2)
- G. W. Wensch
- Reports and Statistics Branch

U. S. Atomic Energy Commission, National Laboratories
- F. Foote, Argonne National Laboratory
- H. Young, Argonne National Laboratory (4)
- E. Childs, Dow Chemical Company
- E. A. Eschbach, Hanford Atomic Products Operations
- E. A. Evans, Hanford Atomic Products Operations
- O. J. Wick, Hanford Atomic Products Operations
- J. Musser, Hanford Atomic Products Operations
- I. D. Thomas, Hanford Atomic Products Operations
- W. Cashin, Knolls Atomic Power Laboratory
- H. Rizzo, Lawrence Radiation Laboratory
- R. D. Baker, Los Alamos Scientific Laboratory
- L. B. Jones, Mound Laboratory
- R. L. Mettler, Oak Ridge National Laboratory (3)
- D. F. Cope, Oak Ridge National Laboratory
- E. S. Bomar, Oak Ridge National Laboratory
- E. J. Kreh, Westinghouse-Bettis Atomic Power Laboratory

U. S. Atomic Energy Commission, Contractors
- R. W. Dayton, Battelle Memorial Institute
- R. F. Dickerson, Battelle Memorial Institute
- G. M. Butler, Jr., Carborundum Company
- K. Taylor, Carborundum Company
- A. D. Schwope, Clevite Research Center
- W. Alter, Vallecitos Atomic Power Laboratory
- K. Cohen, General Electric Company-San Jose
- L. D. Harris, National Carbon Company
- A. Strasser, Nuclear Development Corporation of America
- R. W. Hartwell, Power Reactor Development Company
- D. E. Hamby, Union Carbide Metals Company

NUMEC Distribution

R. J. Atkins
E. M. Benson
F. M. Cain
C. S. Caldwell
J. D. Clement
J. Eck
G. G. Ehrlich
F. Forscher
H. J. Garber
R. W. Gerrish
J. Goodman
B. O. Grable
O. S. Gray
E. K. Halteman
S. A. Haram
R. M. Horgos
M. D. Houston
L. J. Jones
W. C. Judd
A. Kasberg
H. W. Krake
J. C. Limpert
D. C. McKissick
J. Marley
O. Menis
J. F. Miles
L. P. Pepkowitz
K. H. Puechl
W. J. Ross
J. Roth
J. Ruzbacki
J. Scott
Z. M. Shapiro
F. Shipko
J. Stoner
R. S. Swain
J. M. Toman
M. M. Turkanis
B. Vondra
L. Weber
A. M. Weis
M. Zambernard
Library

Previous Quarterly Progress Reports issued in this series are:

NUMBER	For the Period Ending
NUMEC P-10	December 31, 1959
NUMEC P-20	March 31, 1960
NUMEC P-30	June 30, 1960
NUMEC P-40	September 30, 1960
NUMEC P-50	December 31, 1960
NUMEC P-60	March 31, 1961
NUMEC P-70	June 30, 1961
NUMEC P-80	September 30, 1961
NUMEC P-90	December 31, 1961
NUMEC P-100	March 31, 1962
NUMEC P-101	June 30, 1962
NUMEC P-102	September 30, 1962

TABLE OF CONTENTS

PROJECT AND FACILITY ADMINISTRATION

Task 1.00
K. H. Puechl

Summary of Development Activities

During this reporting period, plutonium dioxide was prepared by both oxalate and hydroxide precipitation, and the product powder characteristics were determined. Further, the powders produced by hydroxide precipitation were pressed and sintered. Mixed oxides of UO_2-PuO_2 were also prepared by coprecipitation to supplement and verify results obtained previously. Sintering studies on UO_2-35 w/o PuO_2 prepared by coprecipitation indicated that high density could not be achieved under "normal" sintering conditions. Complete melting of particles composed of UO_2-20 w/o PuO_2 was achieved in the plasma torch, thereby forming good spherical shapes. Torch conditions required to achieve such spheroidization were significantly different than those used previously for the spheroidization of PuO_2 particles. Fabrication of fuel elements for short-term irradiation testing has been continued and is nearing completion. The thermal conductivity of UO_2 has been determined up to a temperature of 1852°C using the point source apparatus. These results are somewhat higher than those measured at other installations but are sufficient proof of the feasibility of the method and essential usefulness of the apparatus.

PuO_2 was produced via oxalate precipitation to determine the effect of plutonium concentration in the feed solution and also to determine the degree of conversion of oxalate to oxide during precipitate drying at room temperature and at 180°C. For both feed concentrations utilized, the results indicate good filterability; i.e., low plutonium losses in the filtrates. Appreciable conversion to PuO_2 was noted on air drying at 180°C; however, little or no conversion was observed at room temperature.

A small lot of PuO_2 prepared via hydroxide precipitation exhibited different powder characteristics from a similar lot prepared previously under seemingly identical conditions. Sintering trials indicated similar lack of reproducibility. Photomicrographs of the sintered pellets from both lots of material indicate that there is a possible relationship between high sintered density and the presence of an, as yet unidentified, gray fused phase along the grain boundaries.

Preparation of UO_2-PuO_2 by coprecipitation has shown that UO_2-12.5 w/o PuO_2 characteristics are not strongly dependent upon ammonia reactant concentration. These results are contrary to results obtained previously with UO_2-20 w/o PuO_2, therefore indicating either a dependence on plutonium composition or a complicated relationship that is not amenable to rationalization without more extensive research.

Sintering of UO_2-35 w/o PuO_2 material prepared by coprecipitation has been continued. The results obtained during this period generally substantiate those obtained previously. It is concluded that high sintered density is more difficult to achieve with this composition than with oxide mixtures containing less plutonium. The relatively low densities achieved appear to be related to small grain size.

Spherical particles of UO_2-20 w/o PuO_2 have been produced by plasma torch fusion using helium torch and carrier gas. Although essentially 100% spheroidization was achieved, central voids were observed in the majority of spheres. Since this phenomenon was noted in early PuO_2 spheroidization trials, it is believed that high density will be attained under more appropriate torch operating conditions.

The apparatus for the measurement of the thermal conductivity of poor conductors at high temperatures is now operational. Test results on a UO_2 sample have yielded thermal conductivity over the range 900-1850°C. The results are somewhat higher than obtained at other laboratories. This may be due to differences in sample characteristics or to inadequacy of the mathematical model for description of the experimental conditions. It has been concluded that the apparatus, as now operating, cannot be further modified to achieve more mathematically ideal conditions. Hence, preparations are being made to commit the apparatus to plutonium use following a more extensive set of calibration measurements.

Composite pellets composed of various compositions of UO_2-PuO_2 and inert cladding and dispersion element matrix materials are being pressed and sintered to allow determination of possible reaction. Reaction effects will be determined by X-ray diffraction and metallography analysis.

Most of the fuel elements for the short-term irradiation tests have been decontaminated and removed from the glove box line. These elements are now undergoing final encapsulation. Continued effort is being placed on the outfitting of the hot-cell alpha boxes required for post-irradiation examination of these test specimens.

Physics studies on near-thermal reactor systems are being extended to higher plutonium loadings. A program has also been initiated to determine the comparative worth of plutonium isotopes in fast reactor systems.

General Plant and Project Aspects

The swager and associated equipment is now completely installed in a glove box. Trial operations with UO_2 will be initiated shortly.

The high temperature dilatometer has been operated satisfactorily to 1000°C using tantalum test samples. This equipment is installed in a glove box and can be committed to plutonium in the near future.

Contract negotiations with the General Electric Testing Reactor are not yet completed; however, all major obstacles have now been resolved. The flow directors and test specimens will be shipped to the reactor as soon as AEC approval of the negotiated contract is received.

PREPARATION AND CHARACTERIZATION OF FUEL MATERIALS

Task 2.00

C. S. Caldwell O. Menis

Preparation and Characterization of Plutonium Oxide
(G. Ehrlich, J. Goodman)

Plutonium oxide has been prepared both by oxalate and hydroxide precipitation. The additional oxalate runs were carried out to determine the effects of feed concentration on final PuO_2 powder characteristics. The hydroxide runs were small-lot preliminary runs to allow general assessment of the properties of PuO_2 powders produced via this route.

Plutonium Oxalate Preparation Route

In order to determine the effects of feed concentration on the properties of PuO_2 prepared by the oxalate method, four additional runs (2 continuous and 2 batch) were completed during this reporting period. Preparation conditions for these are shown in Table 2.1. The conditions for the two continuous runs were essentially those described earlier,[i] as were the conditions for one of the batch runs.[ii] The other batch run, 99-17-6, was carried out by rapidly adding 1.0 M oxalic acid-0.4 M hydrogen peroxide solution to boiling, stirred plutonium nitrate solution and thereby to obtain a 100 per cent molar excess of oxalic acid. Following such addition, the solution was maintained at reflux, and stirring was continued for 16 hours. Following cooldown, the precipitated plutonium oxalate was collected on Mipor polyethylene filter media and allowed to air-dry on the filter for two weeks at ambient temperature. Complete conversion of the dry plutonium oxalate to PuO_2 was then carried out by the standard method.

The feed solutions for the continuous runs, 297Pu26 and 297Pu27A, contained 100 and 194 gm Pu/l, resp. For both cases, the precipitated plutonium oxalate had good filtration characteristics; the filtrates were faintly tan colored and clear, indicating the presence of little or no suspended material. The plutonium content of the filtrates is being assayed to ascertain process losses. The crude filter cakes were washed by drawing one liter of deionized water through the filter cannister. The washed precipitates were air-dried in a forced convection oven at 180°C.

(i) NUMEC P-70, Progress Report, "Development of Plutonium-Bearing Fuel Materials", page 9.

(ii) NUMEC P-60, Progress Report, "Development of Plutonium-Bearing Fuel Materials", page 10.

Table 2.1

Summary of Process Conditions
Plutonium Oxalate Preparation Route

Sample Identification	297Pu26	297Pu27A	297Pu27B	99-17-6
Precipitation Conditions Method Temperature, °C	 Continuous 35	 Continuous 35	 Batch 35	 Batch 100
Feed Composition gm Pu/l H^+, Molarity	 100 3	 194 3	 200 3	 100 3
Strike Solution Composition $H_2C_2O_4$, Molarity H_2O_2, Molarity	(72% Excess) 1.0 0.8	(25% Excess) 1.0 0.8	(25% Excess) 1.0 0.8	(100% Excess) 1.0 0.4
Precipitation Average Holdup, hours	 0.5	 0.5	 0.5*	 16*
Total Number Throughputs	12	8	-	-
Drying Temperature, °C	180	180	180	Ambient
Furnace Conversion Conditions Temperature, °C Time, minutes	 760 30	 760 30	 760 30	 850 15

* Digestion time after completion of oxalic acid addition.

Following normal procedures, air-dried materials were converted to PuO_2 by calcination at elevated temperatures in a static air atmosphere. It was found that the oxalate materials dried at 180°C experienced rather small weight losses upon further heating in air at 760°C, indicating conversion to PuO_2 during the drying operation.

A sample of plutonium oxalate air-dried at ambient temperature for 27 days showed an apparent composition of plutonium IV oxalate containing from 1 to 2 moles of water per mole of plutonium, based on conversion to PuO_2. In Table 2.2 are shown data for seven preparations of plutonium oxalate dried at 180 ± 10°C for various lengths of time. The percentage decomposition was calculated on the basis of dried undecomposed material having the composition $Pu(C_2O_4)_2$ and decomposed material having the composition PuO_2. As can be seen from the calculated decomposition percentages, a significant amount of decomposition occurs as the drying time is extended. These data show that plutonium oxalate is 94-98% decomposed to PuO_2 after drying at 180 ± 10°C for 16 hours. As expected, the decomposition rate was slower for larger drying batches. Although the calculations were based on assumptions regarding chemical forms, the same general conclusions are valid independent of these assumptions.

Measured characteristics of the PuO_2 powders are presented in Table 2.3. The measured surface area of 297Pu26 powder is very close to that of 297Pu27A powder while the surface area of 297Pu27B, the batch-produced material, is 35% higher than either of the other values. Referring to a graph presented earlier,(i) it is seen that the 5.5 M^2/gm surface area of the powder produced in run 297Pu26 corresponds to the expected value (30 minute calcination hold time at 760°C, 100 gm Pu/l feed).

The particle size data obtained with the Mine Safety centrifuge showed rather striking differences between the continuously-produced samples and the batch-produced material. Particle size distribution data presented in Figure 2.1 show that the powders produced from the continuously precipitated precursors contain larger aggregates than the powders produced from the batch produced oxalate. The higher percentage of smaller agglomerates may in part account for the higher surface area of the 297Pu27B preparation.

Plutonium Hydroxide Preparation Route

Details of the preparation of plutonium IV hydroxide by the rapid addition of ammonia to a plutonium IV nitrate solution, followed by long aging with

---

(i) NUMEC P-90, Progress Report, "Development of Plutonium-Bearing Fuel Materials", page 11.

Table 2.2

Thermal Decomposition of Plutonium Oxalate
Dried at 180°C in Forced Air Convection Oven

Sample Number	Pu9-I	Pu9-II	Pu9-III	Pu9-IV	Pu26	Pu27A	Pu27B
Drying Time, hours	6	10	8	8	16	16	16
Weight of Dry Oxalate Charge, gm	326.0	269.5	438.0	271.0	258.6	235.5	258.2
Weight of PuO_2 Recovered, gm	188.6	248.0	362.5	250.5	253.3	233.5	256.2
Weight Loss on Conversion, gm	137.4	21.5	75.5	20.5	5.3	2.0	2.0
Percent Weight Loss	40.8	8.0	17.2	7.6	2.1	0.9	0.8
Calculated Percent Decomposition	None	77.0	50.5	79.1	94.0	97.4	97.7

Table 2.3

Powder Characteristics of PuO_2
Produced via Oxalate Route

Sample	Feed Composition gm Pu/l	Calcination		Bulk Density gm/cc	Tap Density gm/cc	Air Permeability Particle Size, microns	B.E.T. Surface Area M^2/gm	MSA 50% Particle Size microns
		Temp °C	Time min					
297Pu26	100	760	30	2.05	2.85	3.5	5.49	14.0
297Pu27A	194	760	30	1.85	3.09	2.25	5.83	13.0
297Pu27B	200	760	30	1.39	2.83	0.91	7.89	1.7
99-17-6	100	850	15	-	-	-	1.39	-

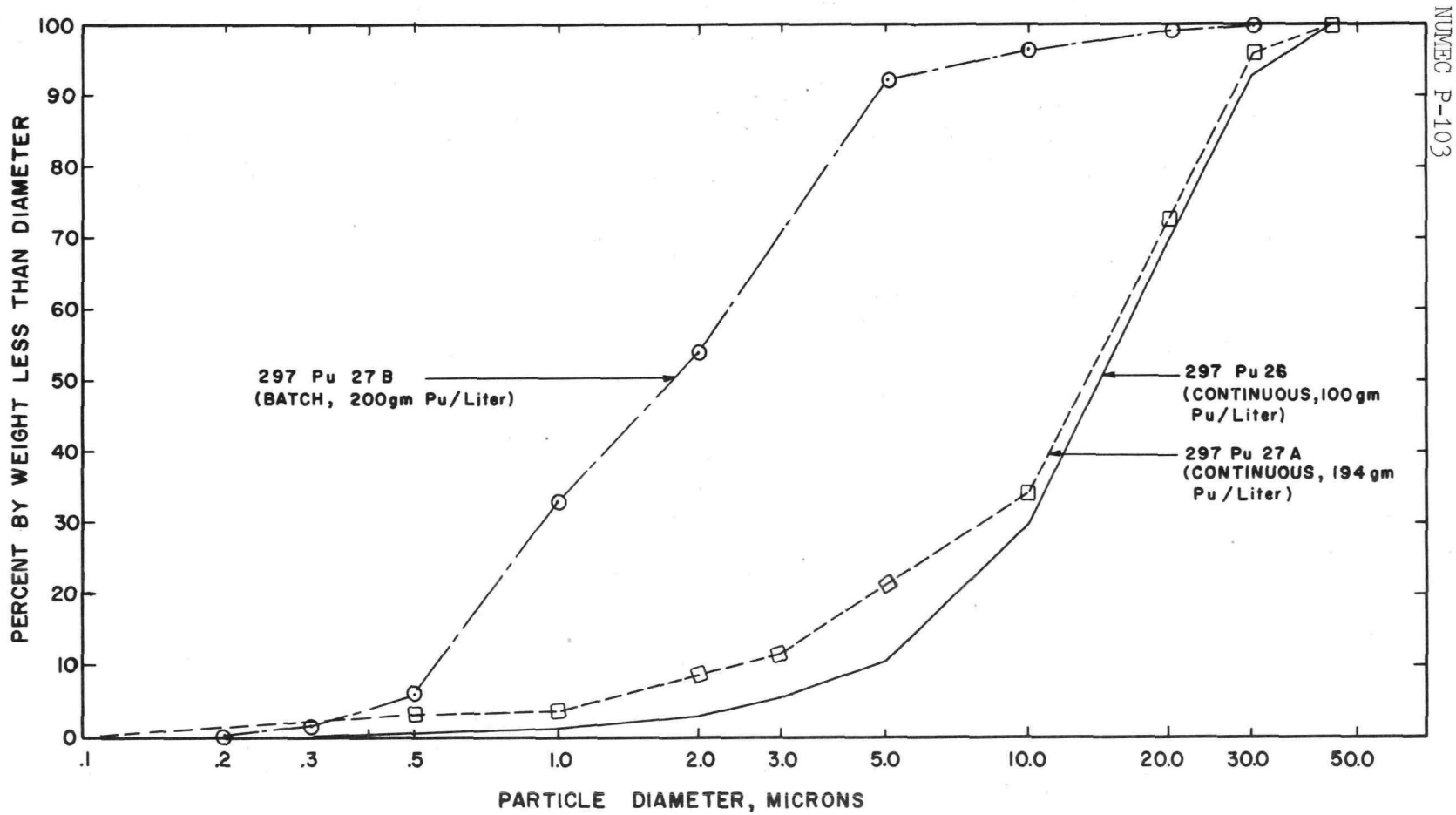

NUMEC P-103

FIGURE 2.1

COMPARISON OF PLUTONIUM DIOXIDE PARTICLE SIZE DISTRIBUTIONS
PREPARED BY BATCH AND CONTINUOUS OXALATE PRECIPITATION
(MSA LIQUID SEDIMENTATION METHOD)

periodic sampling during the aging period were reported earlier.[i] The resultant PuO_2 powder properties did not correlate with the slurry aging time; therefore, a replicate experiment was performed during this reporting period. The sample histories and characterization data for the original and replicate (series 78 and series 17) products are presented in Table 2.4.

From these data, it can be seen that the surface areas of both the intermediate plutonium hydroxide and the final PuO_2 have not been duplicated even though the powders were prepared under apparently identical conditions. Similarly, differences in sintering characteristics were also noted as described under Task 3.00. Further experimentation with larger batches and strict process control is required to clarify these observations.

Complete PuO_2 characterization data have now been obtained for the material prepared previously[ii] by continuous addition of ammonia and plutonium IV nitrate into a stirred precipitator. These data on hammermilled product are presented in Table 2.5. It is seen that the bulk and tap densities are similar to the values associated with material produced by the oxalate route. This observation is also valid for the particle size distribution (presented in Figure 2.2).

Preparation and Characterization of Mixed Plutonium-Uranium Oxides

(G. Ehrlich, J. Goodman)

Two additional continuous coprecipitation runs have been carried out to supplement and verify results obtained previously. The processing procedure for both runs followed the standard method[iii] including precipitate washing by reslurrying. Precipitates produced during the start-up and shut-down portions were segregated as before to provide intercomparisons among materials produced during the various stages of the run. The dried intermediate product from the steady state fractions was thoroughly mixed before preparing furnace charges so that short-term fluctuations in the precipitation step, leading to atypical precursor material, would be averaged out. The preparation conditions for the two runs are presented in Table 2.6. Powder property data including oxygen/metal ratio, B.E.T. surface area, bulk density, tap density, Fisher subsieve particle size, and MSA average particle size are shown in Table 2.7.

Since earlier observations with UO_2-20 w/o PuO_2 powders had indicated that the precursor prepared by using 3.5 M NH_4OH as precipitant was more resistant to heat treatment than precursor prepared with 14.5 M NH_4OH, a similar comparison was carried out under identical conditions used in Run 297Pu20

(i) NUMEC P-102, Progress Report, "Development of Plutonium-Bearing Fuel Materials", page 17.

(ii) NUMEC P-102, Progress Report, "Development of Plutonium-Bearing Fuel Materials", page 19.

(iii) NUMEC P-80, P-90, P-100, P-101, P-102, Progress Report, "Development of Plutonium-Bearing Fuel Materials"

Table 2.4

Conversion Data and Product Characteristics
Plutonium (IV) Hydroxide and Plutonium Dioxide
(Rapid Addition of Concentrated NH_4OH)

Sample Number	Aging Time hours	Pu Assay* of Intermediate % Pu	Surface Area of Intermediate M^2/gm	Calcination Temperature ^oC	Calcination Time hours	Surface Area of Final PuO_2 Product M^2/gm
78-38-1-10	0.16	74.5	33.4	850	2	5.0
17-8-1-10	0.16	-	86.2	850	2	5.7
78-38-1-24	24	78.7	52.3	850	2	20.5
17-8-1-24	24	-	10.3	850	2	8.1
78-38-1-48	48	76.4	37.6	850	2	7.5
17-8-1-48	48	-	40.1	850	2	11.1
78-38-1-72	72	81.3	52.2	850	2	22.2
17-8-1-72	72	-	56.6	850	2	11.2

* The theoretical plutonium content of $Pu(OH)_4$ is 77.9% Pu.

Table 2.5

Characterization Data
for Plutonium Hydroxide and Product Plutonium Dioxide

(Continuous Addition of Reactants)

Sample Number	78-46-27 $Pu(OH)_4$	78-46-27 PuO_2
Pu Assay, w/o Pu	79.8	-
Surface Area, M^2/gm	-	28.4
Bulk Density, gm/cc	-	1.84
Tap Density, gm/cc	-	3.36
Fisher Sub-Sieve Size, microns	-	1.07
Average MSA Particle Size, microns	-	4.4
w/o > 74 microns (200 mesh)	-	2

Table 2.6A

Summary of Preparation Data
for Coprecipitated UO_2-PuO_2 Materials

Run Identification	297Pu24							
Composition	UO_2-12.5 w/o PuO_2							
Precipitation Conditions Method Temperature, °C	Continuous 55	Continuous 55	Continuous 55	Continuous 55	Continuous 55	Continuous 55	Continuous 55	Continuous 55
Feed Composition gm Pu/liter gm U/liter H^+, molarity	 12.0 81.2 1.0	 12.0 81.2 1.0	 12.0 81.2 1.0	 12.0 81.2 1.0	 12.0 81.2 1.0	 12.0 81.2 1.0	 12.0 81.2 1.0	 12.0 81.2 1.0
Feed Flow Rate, liters/hr	1.2	1.2	1.2	1.2	1.2	1.2	1.2	1.2
Precipitant Composition NH_4OH, molarity	3.5	3.5	3.5	3.5	3.5	3.5	3.5	-
Precipitant Flow Rate liters/hr	1.0	1.0	1.0	1.0	1.0	1.0	1.0	-
Precipitant Average Holdup, minutes	30	30	30	30	30	30	30	30
Total Number Throughputs	3.0	2.6	1.1	2.6	2.6	2.6	2.6	1
Run Period	Startup	Steady State	Steady State	Steady State	Steady State	Steady State	Steady State	Steady State
Oxide Sample Identification	TS80-740	SS80-640	TS0-740	SS80-740	SS120-740	SS160-740	SS80-840	RS80-740
Drying Temperature, °C	180	180	100	180	180	180	180	180
Gas Atmosphere	N_2-6% H_2	N_2-6% H_2	N_2-6% H_2	N_2-6% H_2	N_2-6% H_2	N_2-6% H_2	N_2-6% H_2	N_2-6% H_2
Gas Flow, SCFH	4.5	4.5	4.5	4.5	4.5	4.5	4.5	4.5
Rate of Temperature Climb, °C/min	12	12	12	12	12	12	12	12
Conversion Temperature, °C	740	640	740	740	740	740	840	740
Time at Conversion Temperature, minutes	80	80	0	80	120	160	80	80
Furnace Charge, gm	150.9	180	81.5	180	180	180	180	68

Table 2.6B

Summary of Preparation Data
for Coprecipitated UO_2-PuO_2 Materials

Run Identification	297Pu25					
Composition	UO_2-20 w/o PuO_2					
Precipitation Conditions Method Temperature, °C	Continuous 55	Continuous 55	Continuous 55	Continuous 55	Continuous 55	Continuous 55
Feed Composition gm Pu/liter gm U/liter H^+, molarity	 20.0 80.0 1.0	 20.0 80.0 1.0	 20.0 80.0 1.0	 20.0 80.0 1.0	 20.0 80.0 1.0	 20.0 80.0 1.0
Feed Flow Rate, liters/hr	1.2	1.2	1.2	1.2	1.2	1.2
Precipitant Composition NH_4OH, molarity	14.5	14.5	14.5	14.5	14.5	14.5
Precipitant Flow Rate, liters/hr	0.3	0.3	0.3	0.3	0.3	0.3
Precipitant Average Holdup, minutes	30	30	30	30	30	30
Total Number Throughputs	3	7.1				1
Run Period	Startup	Steady State	Steady State	Steady State	Steady State	Shutdown
Oxide Sample Identification	TS80-740	SS80-640	SS80-740	SS80-840	SS40-940	RS80-740
Drying Temperature, °C	180	180	180	180	180	180
Gas Atmosphere	N_2-6% H_2	N_2-6% H_2	N_2-6% H_2	N_2-6% H_2	N_2-6% H_2	N_2-6% H_2
Gas Flow, SCFH	4.5	4.5	4.5	4.5	4.5	4.5
Rate of Temperature Climb, °C/min	12	12	12	12	12	12
Conversion Temperature, °C	740	640	740	840	940	740
Time at Conversion Temperature, minutes	80	80	80	80	40	80
Furnace Charge, gm	192.5	180.0	180.0	180.0	139.4	80.7

Table 2.7

Summary of Powder Characteristics
for Coprecipitated UO_2-PuO_2 Materials*

Sample Number	Oxygen/Metal Ratio in Uranium Fraction	B.E.T. Surface Area M^2/gm	Bulk Density gm/cc	Tap Density gm/cc	Air Permeability Particle Size microns	Average MSA Particle Size for 200 mesh Fraction microns	w/o Greater Than 74 microns (200 mesh)
297Pu24TS80-740	2.23	8.7	0.72	1.59	0.29	0.8	0.0
297Pu24SS80-640	2.35	13.2	0.80	1.53	0.25	5.0	3.9
297Pu24SS0-740	2.59	12.7	0.62	1.33	0.61	4.0	8.2
297Pu24SS80-740	2.21	7.3	0.75	1.59	0.30	4.0	2.8
297Pu24SS120-740	-	10.1***	1.00	1.68	0.29	3.6	2.2
297Pu24SS160-740	2.21	7.6**	0.91	1.68	0.31	1.2	2.8
297Pu24SS80-840	2.12	6.2	0.86	1.96	0.43	0.8	0.0
297Pu24RS80-740	2.29	9.8	0.70	1.50	0.25	4.0	4.5
297Pu25TS80-740	2.20	9.7	0.93	1.76	0.28	1.8	4.0
297Pu25SS80-640	2.42	12.4	0.70	1.57	0.80	2.6	13.7
297Pu25SS80-740	2.23	9.1	0.64	1.46	0.30	5.3	-
297Pu25SS80-840	2.17	6.0	0.69	1.99	0.35	1.4	10.0
297Pu25SS40-940	2.17	4.5	0.92	1.94	0.41	1.3	11.4
297Pu25RS80-740	2.28	10.8	0.54	1.43	0.29	1.3	13.9

* Powder properties measured for hammermilled powders
** Average of 2 measurements
*** Average of 3 measurements

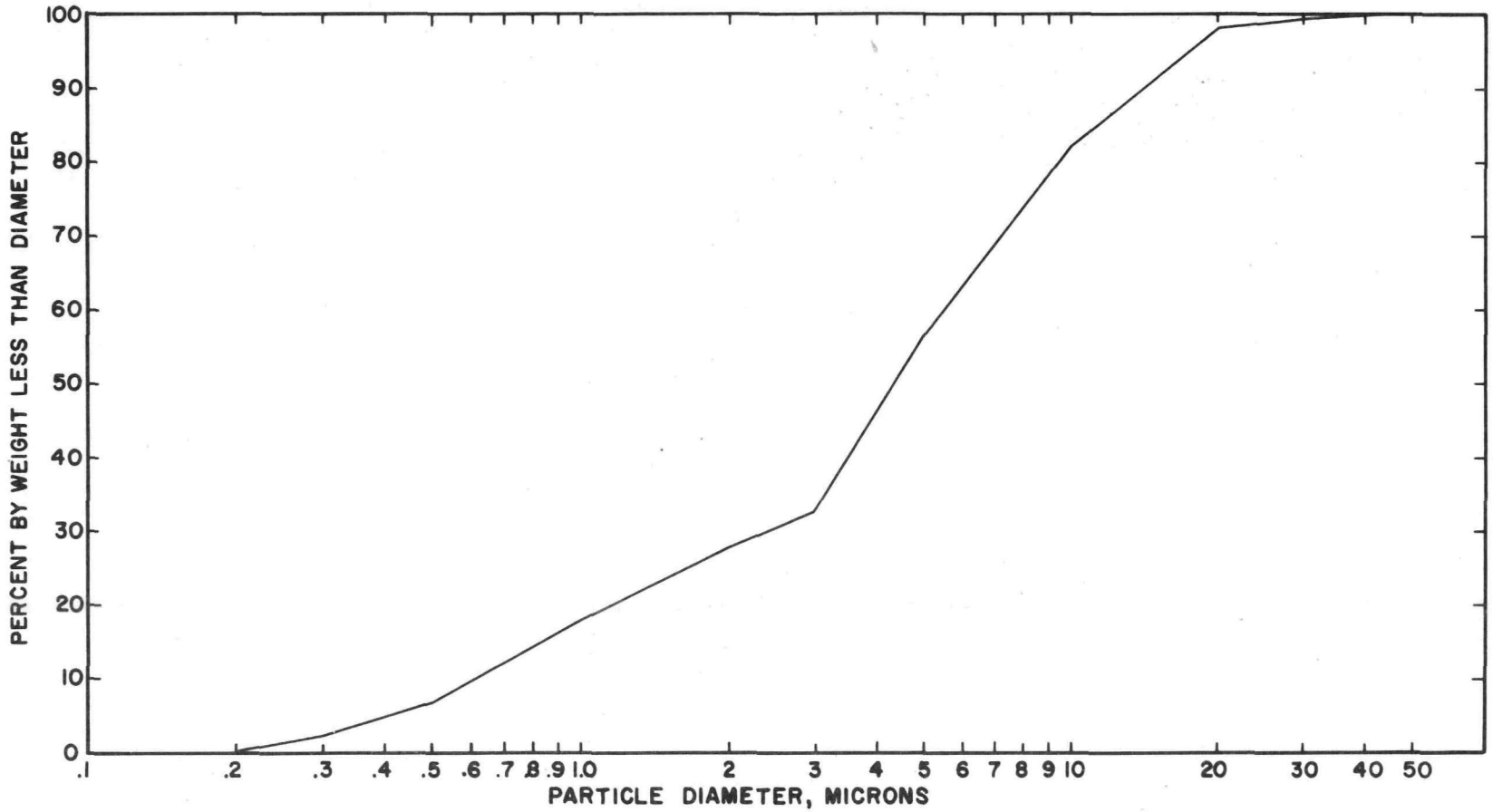

FIGURE 2.2

PARTICLE SIZE DISTRIBUTION OF HAMMERMILLED
PuO_2 DERIVED FROM CONTINUOUSLY
PRECIPATED PLUTONIUM (IV) HYDROXIDE
(MSA LIQUID SEDIMENTATION METHOD)

except that the ammonia concentration was reduced to 3.5 M. A summary of the powder characteristics of the UO_2-PuO_2 product for Run 297Pu24 are presented in Table 2.7. Comparison of these powder properties with those observed on the earlier Run 297Pu20 powders is shown in Table 2.8.

For these steady state comparisons, it is seen that the surface area of the powders produced at various conversion temperatures, at a hold time of 80 minutes at temperature, is not affected by the ammonia concentration. The slight differences in bulk properties for these samples are probably due to variations in hammermilling and therefore cannot be considered effects due to reactant concentration. This observation, that ammonia concentration has a negligible effect on oxide product surface area (for 80 minute conversion time only), is contrary to the results obtained previously with UO_2-20 w/o PuO_2 preparations. Additional verifying runs will be necessary to determine that this difference is inherently due to plutonium content. Comparison of specimens converted at 740°C at varying hold times at temperature, however, does indicate that the ammonia concentration has some influence on the final UO_2-PuO_2 surface area. Specifically, it is to be noted that for the 297Pu20 preparation, the surface area decreased smoothly from 7.6 M^2/gm at 80 minutes hold time to 6.9 M^2/gm at 120 minutes hold time to 6.0 M^2 gm at 160 minutes hold time while for the 297Pu24 preparation, the surface area was a maximum of 10.1 M^2/gm at a hold time of 120 minutes. Since this latter variation appeared to be anomalous, duplicate surface area measurements were performed, and these yielded the same result. It can be concluded that the influence of ammonia concentration on oxide product characteristics is complicated; hence, that generalization is not possible with a small number of preparation runs.

Material prepared in Runs 297Pu24 was also used to study limiting hold time conditions. Samples of the intermediate were rapidly heated to 740°C and then immediately cooled to room temperature at the maximum rate dictated by equipment limitations. It was found that little conversion occurred during this cycle (O/M ratio in uranium fraction was 2.66), and that the surface area (12.7 M^2/gm) was about that normally attained after 80 minutes hold time at temperature. These results indicate that the conversion process cannot be speeded up significantly under present temperature and atmosphere (N_2-6% H_2) conditions. Significant speedup is probably attainable only with higher conversion temperatures and/or with higher hydrogen content atmospheres.

The results of Run 297Pu25 (UO_2-20 w/o PuO_2) presented in Table 2.7 are in essential agreement with data obtained previously under similar conditions (Runs 297Pu13 and 297Pu17). This run indicates that the preparation procedures can be controlled to give a reproducible product.

Table 2.8

Comparative Powder Characteristics
Showing Effect of Coprecipitation with 3.5 M and 14.5 M Ammonia

Sample Number	Ammonia Concentration M	Milling Treatment After Conversion	Oxygen/Metal Ratio in Uranium Fraction	B.E.T. Surface Area M^2/gm	Bulk Density gm/cc	Tap Density gm/cc	Air Permeability Particle Size microns	Average MSA Particle Size for 200 mesh Fraction microns	w/o Greater Than 74 microns (200 mesh)
Pu20S480-640	14.5	H'milled	2.28	11.7	0.68	1.91	0.30	2.5	3
Pu24S380-640	3.5	H'milled	2.35	13.2	0.80	1.53	0.25	5.0	4
Pu20S380-740	14.5	H'milled	2.21	7.6	0.78	1.99	0.40	1.7	5
Pu24S380-740	3.5	H'milled	2.21	7.3	0.75	1.59	0.30	4.0	3
Pu20S3120-740	14.5	H'milled	2.20	6.9	0.69	2.10	0.37	2.5	5
Pu24S3120-740	3.5	H'milled	-	10.1	1.00	1.68	0.29	3.6	2
Pu20S3160-740	14.5	H'milled	2.18	6.0	0.77	2.30	0.41	1.8	4
Pu24S3160-740	3.5	H'milled	2.21	7.6	0.91	1.68	0.31	1.2	3
Pu20S380-840	14.5	H'milled	2.17	6.8	0.74	2.08	0.40	1.0	2
Pu24S380-840	3.5	H'milled	2.12	6.3	0.86	1.96	0.43	0.8	2

Analytical Chemistry
(O. Menis, W. Judd, J. Limpert)

During this reporting period, further improvements in the precision of the determination of plutonium and uranium in oxide mixtures were made, and a manuscript describing these procedures was submitted for publication to Analytical Chemistry Journal. In addition, spectrographic determination of trace impurities by a carrier method was evaluated. An increase in the determination rate of both of these service analyses was achieved without additional manpower effort.

Using X-ray emission analysis with appropriate calibration curves, plutonium content in uranium-plutonium mixtures in quantities of 1 to 10 mg can now be routinely determined within a coefficient of variation of less than 0.4%; in similar mixtures, the uranium fraction in quantities of 10 to 30 mg can be determined within a coefficient of variation of less than 0.7%.

Using a sample of plutonium metal, our spectrographic results for trace impurities were compared directly with similar results obtained at Hanford. At Hanford a gallium oxide carrier method is used in conjunction with a plutonium standard(i) while we use silver chloride, barium fluoride and graphite mixtures in conjunction with a U_3O_8 standard (NBS Sample 65-1 and 2). The comparison data are presented in Table 2.9. It is seen that agreement is generally good except for nickel. This discrepancy has been previously noted(ii) and attributed to the use of plutonium relative to uranium standards.

Many of the analytical chemistry analyses related to the plutonium materials development program are now performed routinely by laboratory technicians. During the past calendar year approximately 600 samples, requiring over 6,000 separate determinations, were routinely analyzed.

These determinations included uranium, plutonium, carbon, free acid, trace impurities or additives, metal-to-oxygen ratios, alpha and gamma spectrometry. The techniques used included differential spectrophotometry and X-ray emission for the simultaneous determination of plutonium and uranium; coulometric and amperometric determination of plutonium; polarographic determination of uranium; gas evolution method for the determination of carbon; spectrographic carrier distillation for the determination of trace

---

(i) Analytical Technical Manual, Emission Spectrography Methods, Hanford Atomic Products Operations, HW5368, February 1961.

(ii) Analytical Technical Manual, Emission Spectrography Methods, Hanford Atomic Products Operations, HW5368, February 1961, page 28.

Table 2.9

Comparison of Spectrographic Chemical Analysis
on Plutonium Metal Sample
(parts per million)

Sample Number	1		2	
Laboratory	NUMEC	Hanford	NUMEC	Hanford
Fe	130	141	150	<250
B	< 1	-	2	-
Co	-	-	-	-
Cd	5	-	10	-
Mn	50	10	30	10
W	10	-	0	-
Al	-	-	-	10
Mg	50	50	20	50
Zn	-	-	-	-
Sn	10	-	<5	10
Cu	10	5	5	25
Pb	<10	2	10	10
Cr	20	10	30	25
Si	10	5	8	< 5
Ti	-	-	0	-
Ni	10	20	20	100
Mo	15	-	<5	10
V	0	-	0	-
Ag	-	1	-	< 5
Ca	-	8	-	5
Na	-	2	-	50

impurities; alpha and gamma counting for the determination of plutonium in solutions; gravimetric analysis for the determination of oxygen-to-metal rations; potentiometric free acid titrations; and volumetric uranium determinations. Constant surveillance of techniques is required to improve accuracy and to minimize labor effort.

FABRICATION AND EVALUATION OF FUEL SHAPES

Task 3.00

E. K. Halteman L. J. Jones

PuO_2 Sintering Studies

(M. D. Houston)

Evaluation of the sintering characteristics of PuO_2 prepared by the hydroxide route has been continued. As shown in Table 3.1, the sintered densities of pellets made from a second batch of hydroxide-precipitated PuO_2, designated 17-8-1, were relatively low (80-86% T.D.) and appeared to be independent of the aging time after precipitation or the sintering atmosphere. This low density is contrasted to the higher densities (92-93% T.D.) reported previously[i] for similar hydroxide-precipitated PuO_2, designated 78-38-1. Furthermore, the microstructures of the two series are quite different. These differences in structure and sinterability cannot be explained at this time; however, these results were not entirely unexpected in view of the differences noted in the characteristics of the two powders (see Table 2.4).

As reported previously,[ii] the microstructures for the higher density compacts of Series 78 consisted of three phases: (a) a matrix of plutonium dioxide grains, (b) a reduced phase, presumably plutonium sesquioxide, present as wide laths across the grains, and (c) a gray fused material, as yet unidentified, along the grain boundaries. The microstructures of all compacts of Series 17, Figure 3.1, failed to show this latter phase, and relatively small amounts of the reduced phase appeared as laths across the grains. It may be significant that the one sample of Series 78 that was aged for only 10 minutes behaved similar to all the samples in Series 17; i.e., this sample sintered to low density and did not show the presence of a third phase. It appears, therefore, that the presence of this third phase and the attainment of high density are inter-related. If this third phase is a liquid at the sintering temperature, then this relationship is probably real and not fortuitous.

Mixed Oxide Sintering Studies

The investigation of the sintering characteristics of UO_2-35 w/o PuO_2 prepared by continuous coprecipitation from the oxalate has been extended

---

(i) NUMEC P-102, Progress Report, "Development of Plutonium-Bearing Fuel Materials", page 29.

(ii) NUMEC P-102, Progress Report, "Development of Plutonium-Bearing Fuel Materials", page 33.

Table 3.1

Sintering Data for Hydroxide-Prepared PuO_2
(Compaction Pressure - 32 TSI; Sintering Temperature - 1600°C)

Composition Designation	Aging Time hours	Green Density gm/cc	Sintering Atmosphere	Firing Weight Loss %	Compact Shrinkage %	Sintered Density gm/cc	Percent of Theoretical Density
17-8-1	0.16	7.73	Air	0.7	7.2	9.57	83.5
17-8-1	0.16	7.81	N_2-6% H_2	1.1	6.7	9.50	82.9
17-8-1	24	7.04	Air	0.6	8.7	9.22	80.4
17-8-1	24	7.01	N_2-6% H_2	1.2	10.2	9.55	83.3
17-8-1	48	7.00	Air	0.7	10.5	9.82	85.7
17-8-1	48	7.00	N_2-6% H_2	1.4	10.4	9.65	84.2
17-8-1	72	6.90	Air	0.7	11.3	9.85	85.9
17-8-1	72	6.75	N_2-6% H_2	1.3	11.7	9.70	84.6

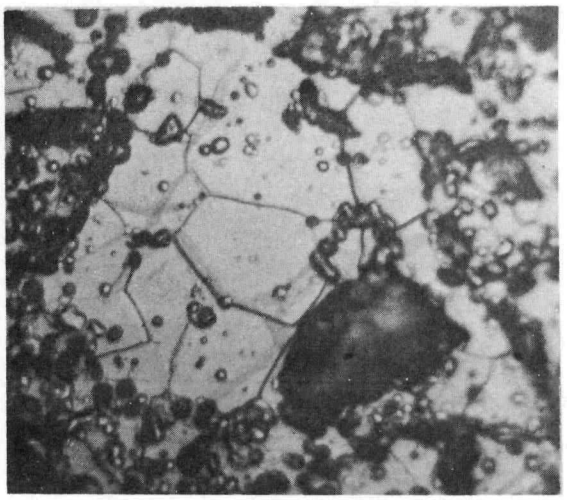

a) Aging Time - 10 minutes
Neg. 413 400X

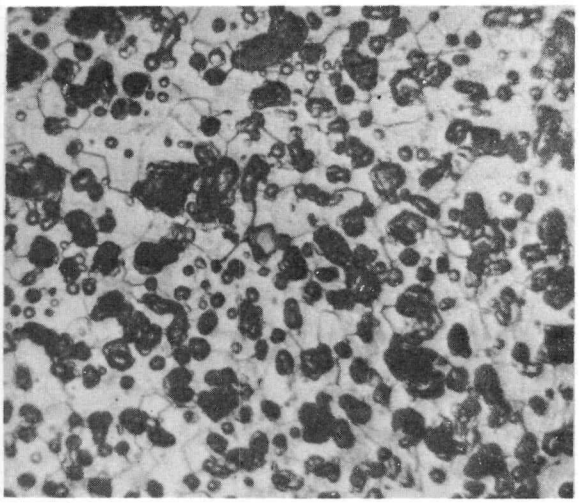

b) Aging Time - 24 Hours
Neg. 414 400X

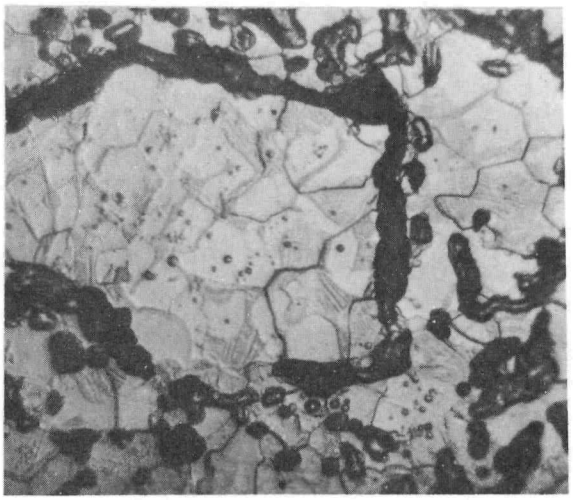

c) Aging Time - 48 Hours
Neg. 415 400X

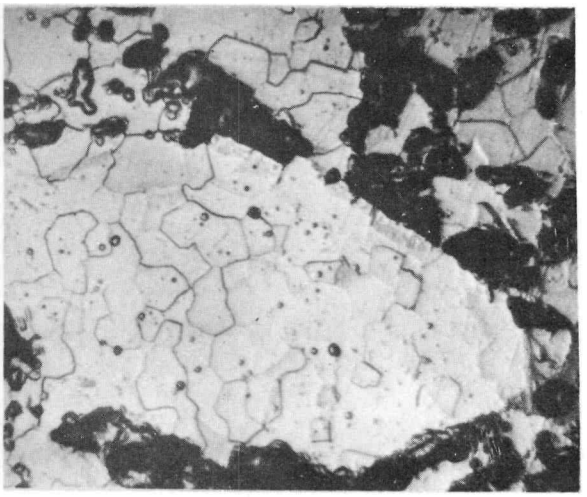

d) Aging Time - 72 Hours
Neg. 416 400X

Figure 3.1

Photomicrographs of PuO_2 Prepared from $Pu(OH)_4$
Compaction Pressure - 32 TSI
Sintered in N_2-6% H_2 at 1600°C for 1 Hour

to include material from the initial transient state (TS) and the residual or terminal state (RS) of the coprecipitation process. The results for the steady state (SS) portion of this material as a function of calcination temperature and time have been previously reported.(i) These previously reported studies indicated that sintered densities in excess of 90% theoretical could be obtained only by long sintering cycles. In Figure 3.2 is shown the microstructure of such a compact sintered for one hour; this reveals the extremely small grain size. The data for the transient and residual state material presented in Table 3.2 show the same sintering characteristics. From these data, it appears that the optimum sintering time is between 1 and 16 hours since longer sintering periods did not result in increased density. These compacts are currently being examined metallographically to establish grain growth as a function of sintering time.

Short-Term Irradiation Test Fuel Fabrication

(M. D. Houston, M. Zambernard)

During this period, twenty additional fuel elements were loaded and tested, bringing to sixty-five the number which have been loaded and hydroformed. These elements will be utilized for both the in-pile specimens and library samples.

The simultaneous hydroforming and leak testing consisted of exposing the welded elements to water in an autoclave at 680°F and 2750 psi for 24 hours. Unannealed Type 316 Stainless Steel tubes showed no deformation whatsoever under these conditions. After annealing in an inert atmosphere at 1000°C for 1 hour, the same tubes deformed readily to the contour of the pellets. It was found that clearances between the pellets and tube wall in excess of 0.002 inch resulted in excess deformation of the tube with clearances above 0.004 inch resulting in folding of the tube wall.

Seven of the sixty-five elements failed to pass the autoclave leak test; weight increases of 0.1 to 0.2 gram were noted. The locations of the leaks were found to be random, indicating no particular fault in any of the fabrication procedures. The locations of some of the defects were easily determined by placing the elements in a vacuum at room temperature; other defects were so small that they could only be detected by heating the elements to 200°C in a vacuum.

Production of Spherical Particles by Plasma Torch

(E. M. Benson)

During this period, work was continued on the spheroidization of the mixed oxides of UO_2 and PuO_2, with the goals being increased sphere

---

(i) NUMEC P-102, Progress Report, "Development of Plutonium-Bearing Fuel Materials", page 37.

Table 3.2

Sintering Data
for Coprecipitated Mixed Oxides of UO_2-35% PuO_2
(Compacted at 11.7 TSI; Sintered at 1600°C in N_2-6% H_2)

Composition Designation	Green Density gm/cc	Sintering Time hours	Firing Weight Loss %	Sintered Density gm/cc	Percent of Theoretical Density
Pu19TS80-740	5.73	1	0.7	8.90	80.0
Pu19TS80-740	5.73	16	0.8	10.11	90.8
Pu19TS80-740	5.74	24	0.5	10.10	90.7
Pu19SS80-740	6.31	1	0.8	9.79	88.0
Pu19SS80-740	6.31	20	1.1	10.21	91.7
Pu19RS80-740	5.48	1	1.0	9.60	86.2
Pu19RS80-740	5.53	16	1.0	10.08	90.6
Pu19RS80-740	5.51	24	0.9	10.06	90.4

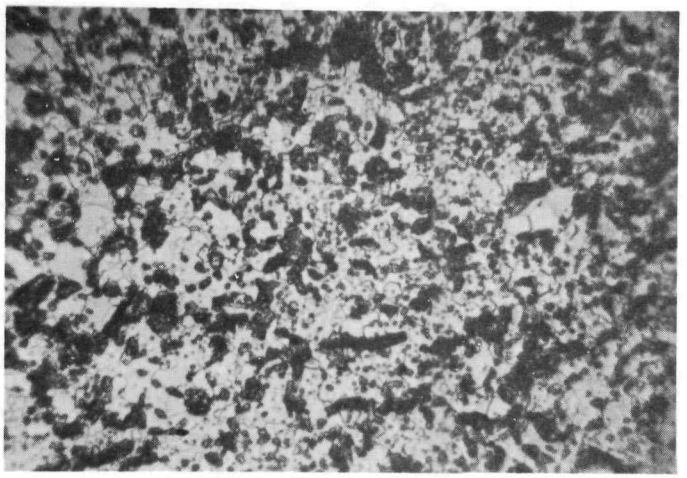

Figure 3.2

Photomicrograph of Coprecipitated UO_2-35 w/o PuO_2
Compacted at 11.7 TSI
Sintered in N_2-6% H_2 at 1600°C for 1 Hour

Neg. 394 400X
C.V.E.

yield and higher density. New feed material, consisting of sintered agglomerates of coprecipitated UO_2-20 w/o PuO_2, was prepared by slug pressing at 2 TSI, manual granulation through a 35 mesh sieve, and sintering in nitrogen-6% hydrogen for one hour at 1650°C. The sintered granules were then crushed and screened into appropriate size ranges. A variety of nozzles (three) and operating conditions were employed. As the nozzle length was increased, the plasma flame varied from turbulant, to laminar, to divergent. Helium and helium-hydrogen gas mixtures at various flow rates and electrical currents were used. The best results, shown in Figure 3.3, were obtained using helium gas and the "standard" F-40 nozzle. The improvement can be seen when compared with earlier results.(i)

Physical Property Measurements
(E. K. Halteman, R. Gerrish, J. Roth)

The apparatus for measurement of the thermal conductivity of poor thermal conductors at high temperature using the point source technique has been successfully operated using UO_2 samples.

Initial measurements were made using electron guns adapted from a 14AP2 television tube. Useful Δt's of 10°C were obtained at the center of the sample at an ambient temperature of 700°C. Calculation of the thermal conductivity from these data gave results which were high by a factor of four from literature values. Much of this discrepancy can be attributed to the fact that at these temperatures the determination of Δt by means of optical pyrometry is difficult because of the low light intensity. However, at higher temperatures, this electron gun could not produce sufficient power in the electron beam to produce measurable Δt's. The apparatus was accordingly modified to accept a higher-power modified Pierce gun. This gun operates with an accelerating potential of 20 kv and is normally used for microwelding. The tungsten filament is capable of emitting 4.5 ma, thereby producing a useful beam power of 90 watts. In contrast, the maximum beam power achieved with the oxide cathode TV electron gun was only 0.4 watt. In order to handle the gas evolution during the initial out-gassing of the boron nitride insulators in the Pierce gun, an auxiliary high vacuum system was also connected to the gun chamber.

After installation of the Pierce gun with its isolated filament power supply, three series of trial runs were completed using UO_2 samples sintered to 90 per cent theoretical density. During the early runs, the emissivities of these samples were not determined due to the difficulty of repositioning the optical pyrometer each time the ambient

---

(i) NUMEC P-102, Progress Report, "Development of Plutonium-Bearing Fuel Materials", page 37.

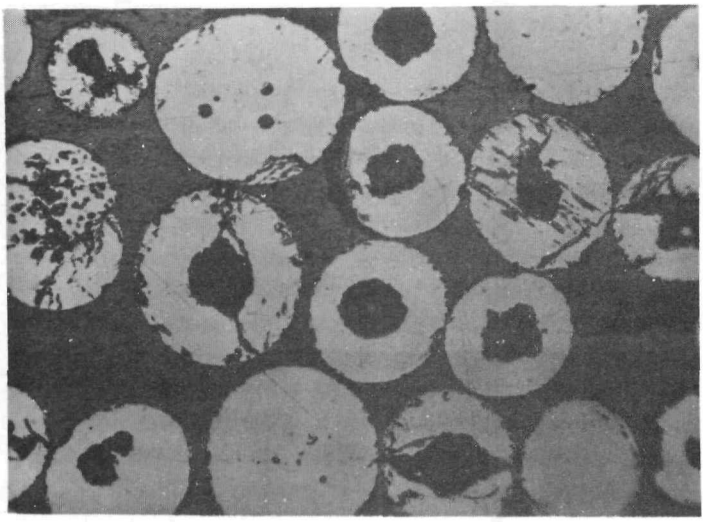

Figure 3.3

Cross-Section of UO_2-20 w/o PuO_2 Spheres
Processed by Plasma Torch

Neg. 390 200X

temperature is changed. (The Δt's are determined by observing the top surface of the sample through a quartz window on the top of the glove box, while the emissivity is determined by observing the hole in the bottom of the sample.) Therefore, the thermal conductivity values were extracted from the data by using values for the emissivity reported by Claudson.[i] These data showed a monotonic decrease in the emissivity from 0.85 at room temperature to 0.37 at 1950°C. The resultant values for the thermal conductivity appeared to be high by more than a factor of 2 when compared to literature values. Powers, et al,[ii] reported a value of 0.81 for the emissivity of a UO_2 surface in the "as-sintered condition" and that the emissivity was independent of temperature. When this value was used for the emissivity, the associated thermal conductivity values were decreased. Finally, the emissivity of actual samples used in the point source apparatus were measured in a separate experiment using the method of Sparron, et al.[iii] These measurements indicated an emissivity of 0.90, independent of temperature. The results of the calculations for extracting the thermal conductivity from the third run data under the various emissivity data are shown in Figure 3.4 along with the thermal conductivity results on UO_2 obtained at other laboratories. It is seen that at 1000°C our results using an emissivity of 0.90 are 50 per cent higher than the value reported by Battelle Memorial Institute. This difference may be due to differences in the character of the UO_2 samples utilized. However, it may also be due to the finite size of the "point" source used in our apparatus. A mathematical analysis of the effect of source size will therefore be undertaken.

The measurements on UO_2 indicate that the apparatus is operable and that reproducible and meaningful results can be obtained. No further modifications to the present apparatus are contemplated; however, accuracy may be improved by refinement of the mathematical analysis of the data. The auxiliary apparati are now being relocated to allow operation with plutonium inside of a glove box. Prior to such operation, additional measurements will be made on "cold" materials to ascertain whether the apparatus can be used for absolute determination of the thermal conductivity or whether it will be operated to generate only comparison data.

(i) T. T. Claudson, "Emissivity Data for Uranium Dioxide", HW-55414, November 5, 1958.

(ii) R. M. Powers, Y. Cavallaro, J. P. Mathern, "The Effects of Solid Solution Additions on the Thermal Conductivity of UO_2", SCNC-317.

(iii) E. M. Sparrow, L. V. Albers, E. R. G. Eckert, "Thermal Radiation Characteristics of Cylindrical Enclosures", Journal of Heat Transfer, 84, 73, 1962.

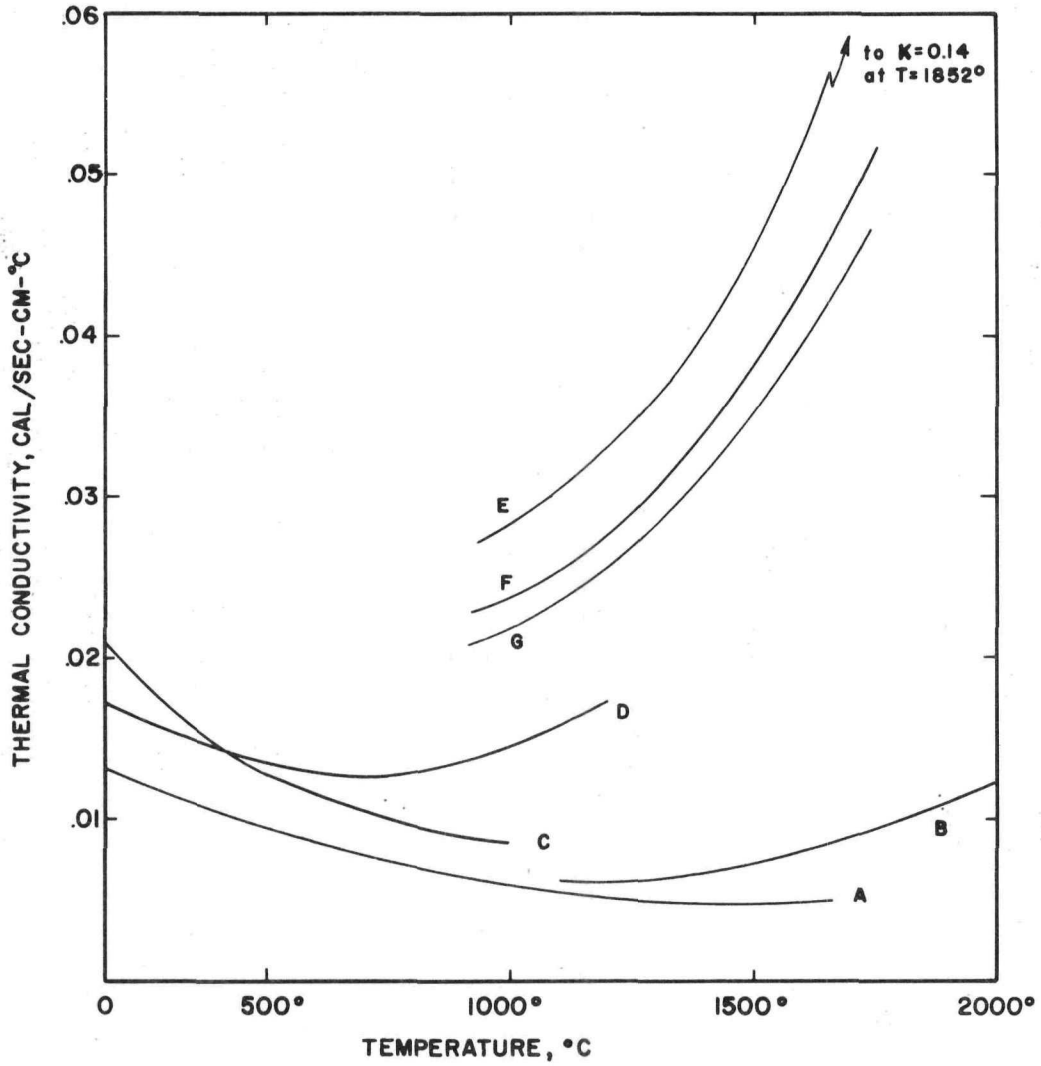

A. HEDGE AND FIELDHOUSE, AECU 3381
B. BATES, NUCLEONICS 19,(6),83,(1961)
C. KINGERY, NYO 3647
D. DEEM AND MATLICH, BMI 1581
E. NUMEC, RUN 3 E=0.85 to 0.37, CLAUDSON, HW 55414
F. NUMEC, RUN 3 E=0.81 POWERS et al, SCNC 317
G. NUMEC, RUN 3 E=0.90 MEASURED

FIGURE 3.4

THERMAL CONDUCTIVITY OF UO_2
USING POINT SOURCE HEAT INPUT

The power supply for the high temperature dilatometer has been tested, and sample temperatures up to 2300°C have been obtained. A linear variable differential transformer and a tungsten/tungsten-rhenium thermocouple has been installed, and the connections through the glove box wall have been made vacuum tight. Preliminary dilatometric tests up to 1000°C were run with a tantalum sample, and results were obtained within the range of literature values. A stepless programmed temperature controller is now being installed to allow control of the input to the power transformer to improve the linearity of the rate of temperature rise.

The installation of an MRC high temperature x-ray camera on a diffractometer within a NUMEC Type "C" glove box has been initiated. When this equipment becomes operational, the time required to obtain x-ray diffraction data will be greatly reduced. Also, when this diffractometer becomes available, the present diffraction arrangement, which currently uses the glancing angle technique, will be adapted to allow the use of the conventional rotating powder method.

FUEL ELEMENT FABRICATION AND EVALUATION

Task 4.00
L. J. Jones

Compatibility Study
(M. Zambernard)

The PuO_2-UO_2 coprecipitated powders containing 0.5, 5, 12.5, 17.8, and 35 w/o PuO_2 have been compacted and sintered, producing satisfactory pellets of 90 to 94% theoretical density. For the compatibility studies, these pellets of fissile material are being surrounded by powdered cladding material compacted in situ. The duplex pellets of the 304 and 316 stainless steels, iron, nickel, chromium, molybdenum, and tungsten have been compacted. Further, the pellets of the stainless steels, iron, nickel, and molybdenum have been sintered and are currently awaiting sectioning and metallographic examination to determine the extent of the reaction at the interface between clad and core. Other cladding material powders, requiring an inert atmosphere, i.e., titanium, niobium, vanadium, Zircaloy-2, and tantalum, are currently being compacted into duplex pellets. In addition, UO_2-80 w/o PuO_2 and pure PuO_2 powders, possible fuel materials for dispersion elements, are being sintered into core pellets. Samples containing 50 v/o fissile and 50 v/o cladding materials, blended together uniformly, are being sintered simultaneously with the duplex pellets in order to provide x-ray diffraction data under identical conditions of temperature and atmosphere.

Corrosion Tests
(M. Zambernard)

Pellets of each of the seven compositions of fissile materials being used in the compatibility study are being pressed and sintered for corrosion testing in 650°F deionized water under equilibirium pressure. Initially, five pellets of each composition will be exposed for periods of 100, 500, and 1000 hours with the weight gain (or loss) checked after each time period. Additional corrosion tests under more stringent conditions will be undertaken after examination of these results.

Equipment Installation
(M. Zambernard, D. McKissick)

The swage box installation is now complete. Trial runs using UO_2 will be initiated shortly prior to commitment to plutonium.

The autoclaves in the glove boxes are being modified prior to initiation of the corrosion study. The stainless steel gaskets have been replaced

with laminated gaskets and over-pressure controls are being added to minimize the probability of rupture-disk blow out since such blow out would require major box clean-up.

RADIATION TESTING AND EVALUATION

Task 5.00
L. J. Jones

Short-Term Irradiation Tests
(R. M. Horgos, L. J. Jones)

Final flux perturbation calculations on the short-term irradiation capsules have been completed at the General Electric Test Reactor (GETR) using a P-3 approximation. These results indicate that the capsules can be irradiated in the $2\frac{1}{2}$ inch Trail Cable Facility without the need for auxiliary flux depressants such as the boron steel that had been considered. Aluminum capsules will therefore be used for all specimens, and minor corrections to the flux will be made by regulation of the vertical position of the capsule within the test hole.

Fabrication of two assemblies of the combination coolant flow director-capsule holder[1] has been completed. The in-pile sections of these assemblies, one unassembled, are shown in Figure 5.1. The removable plug permits loading and unloading of the capsules in the GETR canal.

Fabrication and assembly of the aluminum capsules have been completed to the point of loading the test specimens. Two such capsules, one unassembled, are shown in Figure 5.2, together with three of the stainless steel clad UO_2-PuO_2 fuel elements. Note that, as required by the GETR, two aluminum welds separate the NaK coolant in the capsule from the reactor process cooling water which flows across the surface of the capsule, and an additional stainless steel weld separates the NaK coolant from the fuel.

Forty fuel elements have been successfully decontaminated and removed from the glove box system. From this group, nine of the proposed fourteen capsules can be assembled. It is expected that these nine capsules will be ready for shipment by mid-January. The remaining thirteen elements are duplicates of those being encapsulated and will be retained as library samples. The decontamination procedure utilizes a two-step ultrasonic cleaning procedure. In the first step, a mixture of tartaric and citric acid is used; in the second step, EDTA. Such decontamination has reduced the removable activity to 1000 alpha counts per minute prior to bagging out of the glove box line. A subsequent similar two step ultrasonic cleaning procedure performed in a chemical hood has resulted in a reduction of the removable activity to 50 alpha counts per minute.

(i) NUMEC P-101, Progress Report, "Development of Plutonium-Bearing Fuel Materials", page 35.

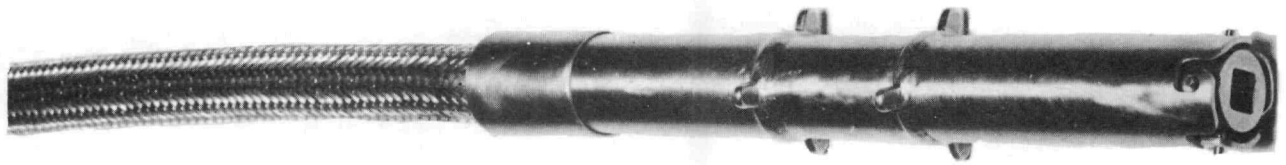

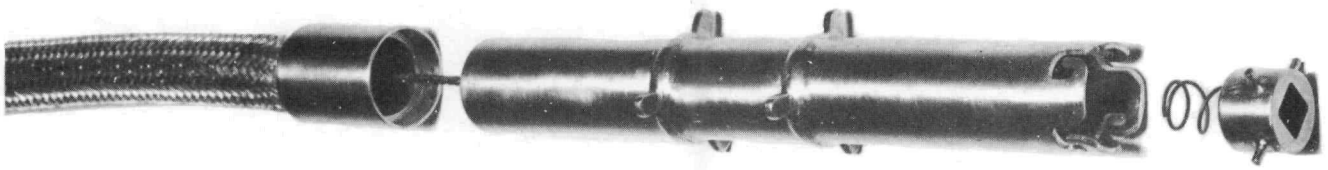

Figure 5.1

Coolant Flow Director
Capsule Holder

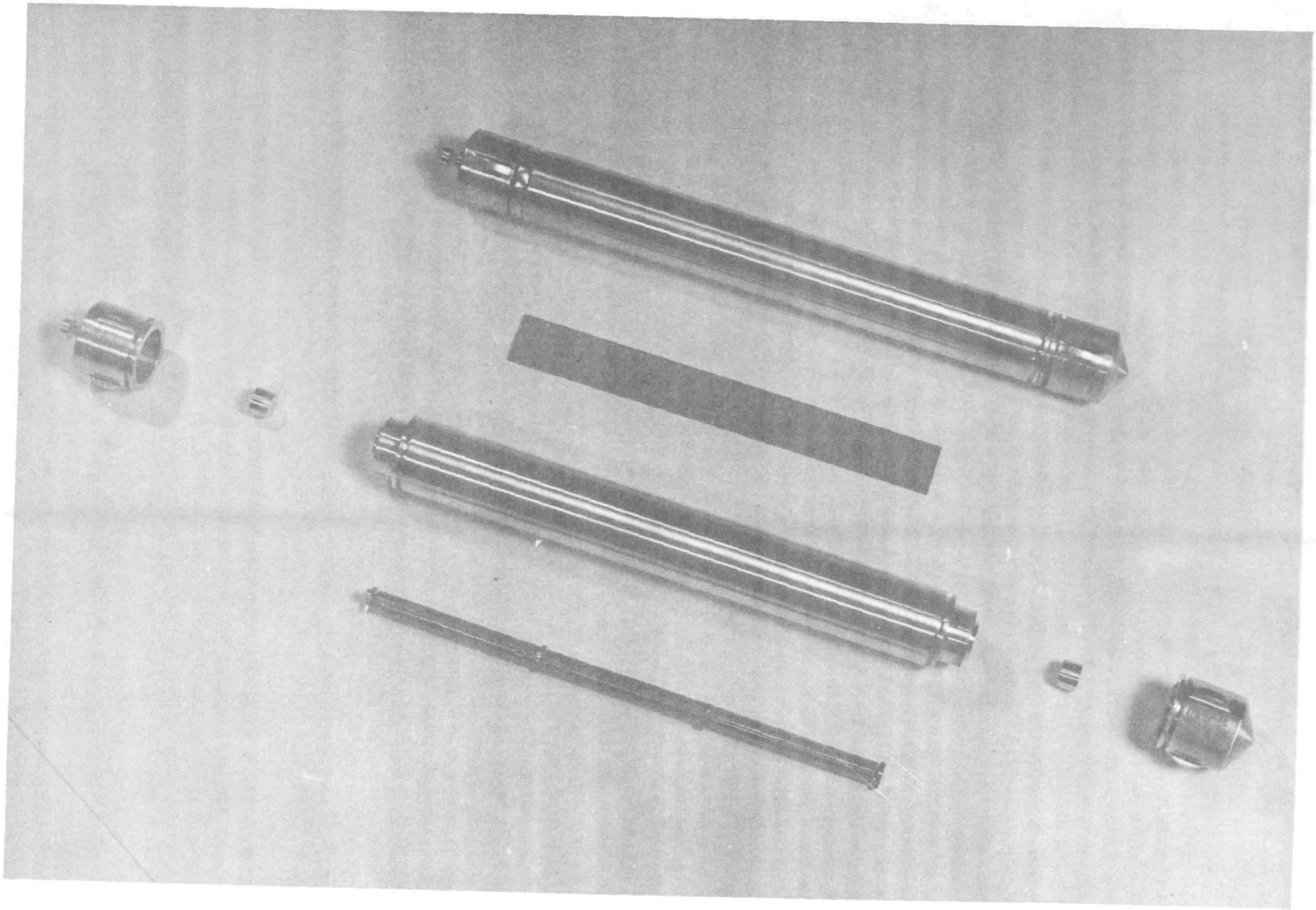

Figure 5.2

Irradiation Test Capsules and Fuel Elements

Hot Laboratory Equipment Fabrication

(R. M. Horgos)

Modifications to the alpha box for the metallographic facility have been completed, including the modification of the Bausch and Lomb metallograph for attachment to this box. Assembly of the enclosure and installation of the metallography equipment has been started.

In order to complete all the operations and evaluations of the short-term irradiation tests, it is anticipated that three hot cell alpha boxes will be required to contain all the necessary equipment. Major emphasis is therefore being placed on completing these three boxes. Two of the alpha boxes have been assembled in order to perform a leak test on the window seals. Since the windows are made of non-browning plate glass, there was some concern about obtaining a gas-tight seal at the window edges; however, both boxes gave indication of a leak rate of less than 0.1 volume per cent per hour, which was the preset design specification. Except for the gamma scanning device, all necessary equipment is on hand and can be readily installed in these boxes.

REACTOR PHYSICS AND ENGINEERING PARAMETRIC STUDIES

Task 8.00
J. D. Clement

Assessment of Plutonium in Near-Thermal Reactors
(W. Ross, J. Ruzbacki)

Reactor physics studies of near-thermal reactors containing plutonium are being extended to include higher plutonium content systems. Since the ratio of plutonium-to-hydrogen atom densities for these systems is generally higher than used previously, the SUFOCATE(i) code is being used to compile an extended tabulation of cross sections for the NUSURP code.

As another check on the NUSURP procedure, a comparison was made between calculated Pu-239 and Pu-241 fission ratios relative to U-235 and Klein's(ii) experimental and calculated values. Table 8.1 shows the comparison. The ratios calculated by Klein were based on fast constants obtained with the MUFT(iii) code.

Comparative Worth of Plutonium Isotopes in Fast Reactors
(J. D. Clement)

A study has been initiated to determine the relative worth of plutonium isotopes in fast reactor systems. Since Pu-240, in particular, is a reasonably good fast fissioning isotope, the value of high burnup plutonium is probably appreciably different in fast reactors than in thermal reactors. The ultimate mode of recycle within a power complex composed of both thermal and fast reactor types is therefore dependent upon the relative value of high burnup plutonium in these two systems.

To date, only limited consideration has been given to this value determination. For example Okrent and Thalgott(iv) tabulate the average

---

(i) H. Amster and R. Suarez, "The Calculation of Thermal Constants Averaged Over a Wigner-Wilkens Flux Spectrum", WAPD-TM-39, (January 1957).

(ii) D. Klein, Nuclear Science and Engineering, 8, No. 5, 405 (1960).

(iii) H. Bohl, Jr., E. M. Gelbard, G. H. Ryan, "MUFT-4-Fast Neutron Spectrum Code for the IBM-704", WAPD-TM-72 (July 1957).

(iv) D. Okrent and F. W. Thalgott, "Physics of Plutonium in Fast Reactors", MTP-566.

reactivity parameter ($\nu\bar{\sigma}_f - \bar{\sigma}_f - \bar{\sigma}_c$) for the various plutonium isotopes in four different fast reactor spectra. Such a tabulation is qualitatively useful; however, it gives little quantitative information regarding relative value of the plutonium isotopes. Even when account is taken of the fissionable daughters formed by neutron absorption, as presented in Table 8.2, the tabulation is still not quantitatively meaningful. What is required to determine value is a broader set of reactor calculations, including the effects of burnup, similar to those which have been carried out on thermal reactor systems. A relatively simple calculation procedure is therefore being developed to allow such assessment by reactor performance and fuel cycle cost comparison.

Table 8.1

Comparison of
Pu-239 and Pu-241 Fission Rates Relative to U-235

	Experimental	Calculated (Klein)	NUSURP
(Water-to-Uranium Ratio 2.35 to 1)			
Pu-239/U-235 Fission Ratio	1.95±.03	1.80	1.80
Pu-241/Pu-239 Fission Ratio	1.18±.03		1.15
(Water-to-Uranium Ratio 1 to 1)			
Pu-239/U-235 Fission Ratio	2.16±.02	2.14	2.08
Pu-241/U-239 Fission Ratio	1.05±.02		1.04

Table 8.2

Average Value of

$$(\nu\sigma_f - \sigma_f - \sigma_c)_{\text{Parent}} + \left(\frac{\sigma_c}{\sigma_c+\sigma_c}\right)_{\text{Parent}} (\nu\sigma_f - \sigma_f - \sigma_c)_{\text{Daughter}}$$

for Various Isotopes in Various Fast Reactor Spectra

Reactor Type Spectrum	U^{238}	Pu^{239}	Pu^{240}	Pu^{241}
EBR-II	2.043	3.566	2.243	4.081
FERMI	2.377	3.471	2.324	4.315
800L Metal	2.702	4.483	3.088	5.160
1500L Oxide	2.701	3.476	3.201	5.259